Simplicial minisuperspace models in the presence of a scalar field

Cristóvão Correia da Silva [1] and *Ruth M. Williams* [2]

DAMTP, Silver Street, Cambridge,
CB3 9EW, England

ABSTRACT

We generalize simplicial minisuperspace models associated with restricting the topology of the universe to be that of a cone over a closed connected combinatorial 3−manifold by considering the presence of a massive scalar field. By restricting all the interior edge lengths and all the boundary edge lengths to be equivalent and the scalar field to be homogenous on the 3−space, we obtain a family of two dimensional models that include some of the most relevant triangulations of the spatial universe. After studying the analytic properties of the action in the space of complex edge lengths we determine its classical extrema. We then obtain steepest descents contours of constant imaginary action passing through Lorentzian classical geometries yielding a convergent wavefunction of the universe, dominated by the contributions coming from these extrema. By considering these contours we justify semiclassical approximations based on those classical solutions, clearly predicting classical spacetime in the late universe. These wavefunctions are then evaluated numerically. For all of the models examined we find wavefunctions predicting Lorentzian oscillatory behaviour in the late universe.

[1]e-mail address : clbc2@damtp.cam.ac.uk
[2]e-mail address : rmw7@damtp.cam.ac.uk

1 Introduction

The quantization of gravity, (QG), is perhaps the most important problem in theoretical physics today. Among the several avenues proposed to achieve that goal, one of the most productive has been the sum over histories formulation. In such a formulation an amplitude for a certain state of the universe is constructed by summing over a certain class of physically distinct histories that satisfy appropriate boundary conditions, weighted by their respective action. Problems with the convergence of the path integral for gravity make it convenient to use the Euclidean version of the sum over histories.

In the (Euclideanized) classical theory of gravity, i.e., general relativity, (GR), a classical history is a Riemannian manifold, that is, a smooth manifold (M^n, A) with smooth structure, (atlas), A, endowed with a Riemannian metric g. Topological manifolds M^n, with their local homoeomorphisms to R^n, are the mathematical implementation of GR's Equivalence Principle. The smooth and metric structures are essential for the definition of the most basic physical concepts like distance, curvature, field derivatives, etc.

When building a quantum version of GR there are several reasons why we should consider the generalisation of this concept of history. Any sum over histories can only be implemented once we specify what are the elements of the set of (physically distinct) histories in QG we have chosen to consider. Such choice is constrained by several criteria that any reasonable history in QG must meet. The most fundamental are:

- It should be based on a finite dimensional topological space X^n endowed with a smooth structure A.
- The above mentioned space must be metrizable.
- The set of physically distinct histories $\{X^n, A, g_{\mu\nu}\}$ considered in the sum must be algorithmically decidable, AD, and classifiable, AC.
- The action functional used should coincide with the usual Einstein action for manifold-based histories.

Given such a set of histories it is then possible to write a probability amplitude for topology change between a set of boundary $(n-1)-$manifolds ∂X^{n-1} in the same cobordism class, as

$$G[\partial X^{n-1}, h] = \sum_{(X^n, A)} \int Dg_{\mu\nu} e^{-I[X^n, A, g_{\mu\nu}]} \tag{1.1}$$

where the sum is over all physically distinct histories, $\{X^n, A, g_{\mu\nu}\}$, that have the appropriate boundaries (∂X^{n-1}), and induce the desired $(n-1)$ metric, h, on those same boundaries, and I is the Euclidean action associated with each history.

Any successful theory of QG must have GR as its low energy limit, and so its space of histories must contain the space of classical, manifold-based histories. However, although necessary there are several indications that they are not sufficient. To start with, the set of $n-$dimensional smooth manifolds is not AC for $n \geq 4$, and there is no known algorithm to decide whether or not a generic topological space is a manifold in 4 dimensions. It was proven there is no way to do so for higher dimensions.

Furthermore, there are cases in which formal descriptions of histories based on the classical configurations of a theory, do not necessarily correspond to the precise mathematical definition of the space of histories needed in order to make Euclidean sums over histories both well defined and yielding the correct quantum mechanics, [1]. On the other hand these histories cannot be based on very pathological topological spaces, because it would be impossible to concretely define the action associated with those generalized topological spaces. This requires the definition of concepts like distance, volume and scalar curvature. In order to define distance, the topological spaces must be metrizable, and it can be shown that a notion of curvature can be introduced in any metrizable space where such notion of distance exists.

However, such spaces must also have uniform dimension, otherwise it would not be clear how to weight their contributions in a sum over histories, since the form and properties of the action depend on the dimension of the space. As pointed out by Scheleich and Witt in [2], these restrictions are still not enough to eliminate all unsatisfactory topological spaces, and they go on to discuss in some detail what other restrictions are necessary.

A good candidate for this generalized space of histories as been suggested in [2]. They propose generalizing from manifold-based histories to conifold-based histories. Briefly a conifold is a topological space that is like a manifold everywhere except in a discrete, countable set of points S, (called singular points), that do not have any neighbourhood homeomorphic to an open ball of R^n, but to a cone over some closed connected $(n-1)-$manifold (other than S^{n-1}, of course).

In one and two dimensions, manifolds and conifolds coincide. But for higher dimensions the set of conifolds more than contains the set of manifolds. The fact that the set of non-manifold like points, S, in any conifold is discrete and countable allows the direct generalization of all basic geometrical concepts, (such as geodesics, curvature, etc.) from manifolds to conifolds by continuation.

The problem now is how to concretely implement such a sum. To do it we must not only define the space of histories we will be considering but also obtain a finite representation for them. A simplicial formulation of QG in terms of Regge calculus aims to provide one such representation. Following [2] by defining combinatorial manifolds and conifolds in the appropriate way, we can be sure that in less than seven dimensions there is a one to one relationship between smooth manifolds/conifolds and their combinatorial counterparts.

These combinatorial counterparts are thus a finite representation of the smooth topological spaces they are associated with. Furthermore this one to one relationship allows us to substitute the sum (1.1) for a sum over those simplicial complexes, which is easier to concretely implement.

However, the computation of the full sum is not at present viable, and so we restrict ourselves to a simplicial minisuperspace approximation for the wavefunction of the universe for some simple but fairly general models. Such calculations were initiated in [3], [4] and extended in [5] and [8]. We aim to further extend these models and verify if they yield a wavefunction predicting classical spacetime.

Our simplicial minisuperspace approximation consists in restricting the topology of the $4-D$ universe to be that of a simplicial cone over a $3-D$ closed connected combinatorial manifold, which is to be seen as a triangulation of the spatial $3-D$ universe. Furthermore, its geometry must be such that there is a single type of boundary edge ,with square length s_b, and internal edge with squared length, s_i. We shall also consider that there is a massive scalar field present, but that it takes the same value in all the vertices of the spatial $3-D$ universe, which is analogous to the requirement of the scalar field to be homogeneous $\phi = \phi(t)$ in the usual continuum minisuperspace models, [10].

As pointed out in [4], we shall see that the only way of obtaining a wavefunction predicting a late universe exhibiting classical spacetime like our own, (i.e. a wavefunction with Lorentzian oscillatory behaviour), is to consider contours of integration over complex valued interior edge lengths, s_i. This forces us to study the minisuperspace action as a function of complex variable, which is rather involved because of the multivaluedness of the action.

We then try to find convergent integration contours yielding appropriate wavefunctions, i.e., that predict Lorentzian classical spacetime in the late universe, by allowing a semiclassical approximation based on Lorentzian classical solutions to be a good approximation of the full wavefunction when the universe is large.

2 Simplicial Quantum Gravity

2.1 Combinatorial Manifolds and Conifolds

Before we introduce our simplicial minisuperspace model it is convenient that we review some basic definitions of simplicial geometry.

Definition 2.1 *A simplicial complex* $(K, \mid K \mid)$ *is a topological space* $\mid K \mid$ *and a collection of simplices* K*,such that*

- $\mid K \mid$ *is a closed subset of some finite dimensional Euclidean space.*
- *If* σ *is a face of a simplex in* K*, then* σ *is also contained in* K*.*
- *If* σ_a *and* σ_b *are simplices in* K*, then* $\sigma_a \cap \sigma_b$ *is a face of both* σ_a *and* σ_b*.*
- *The topological space* $\mid K \mid$ *is the union of all simplices in* K*.*

Definition 2.2 *A combinatorial* $n-$*manifold* $\mathcal{M}^n$*, is an* $n-$*dimensional simplicial complex such that*

- *It is pure.*
- *It is non branching.*
- *Any two* $n-$*simplices can be connected by a sequence of* $n-$*simplices, each intersecting along some* $(n-1)-$*simplex.*
- *The link of every vertex is a combinatorial* $(n-1)-$*sphere.*

Note that there are simplicial complexes that are homeomorphic to topological manifolds but are not combinatorial manifolds. The definition of combinatorial manifold carries more structure than simply the topology. A similar definition can be made for combinatorial conifolds $\mathcal{C}^n$, by simply replacing the previous last condition by

- The link of every vertex of $\mathcal{C}^n$ is a closed connected combinatorial $(n-1)-$manifold.

Thus, like in the continuum framework, a general combinatorial conifold is a combinatorial manifold everywhere except possibly at a countable set of vertices,

Combinatorial manifolds and conifolds are in a similar situation to smooth manifolds and conifolds, in the sense that they both have additional structure relative to their more general topological counterparts. Such structure allows integration and differentiation to be well defined as essential for any physical applications. In order to see the connection between the smooth and combinatorial structures we need to introduce one more definition:

Definition 2.3 *A combinatorial triangulation of a manifold, M^n, consists of a combinatorial manifold $\mathcal{M}^n$, and an homeomorphism $t :| \mathcal{M}^n | \rightarrow M^n$.*

An analogous definition holds for conifolds.

Following [2] it can be shown that every smooth manifold and conifold admit combinatorial triangulations. On the other hand, it can be also shown that every combinatorial manifold admits a piecewise-linear, (PL), structure, i.e. a PL-atlas, $\{(V_a, \phi_a)\}_{a\in A}$, such that the mappings

$$\phi_b \phi_a^{-1} : \phi_a(V_a \cap V_b) \rightarrow \phi_b(V_a \cap V_b) \tag{2.1}$$

are PL mappings between subsets of R^n_+. Finally it is known that in less than seven dimensions every manifold with a PL-structure has an unique smoothing. A similar reasoning can be applied to conifolds, and so we are able to conclude that

In less than seven dimensions, smooth manifolds/conifolds, (M^n/C^n), uniquely correspond to combinatorial manifolds/conifolds, $(\mathcal{M}^n/\mathcal{C}^n)$.

Obviously the topological space underlying each smooth manifold/conifold may have several inequivalent triangulations, what this result says is that when we specify a smooth structure on that space it will correspond to a unique combinatorial triangulation, i.e., a triangulation based on a combinatorial manifold/conifold, and not just any simplicial complex. This unique correspondence implies that in less than seven dimensions the information about the smooth structure of the space is carried by its combinatorial triangulation. So we see that the topological part of the sum over histories in (1.1), can be recast in terms of

simplicial representatives of the "continuum" spaces. However in order to fully translate an heuristic expression such as (1.1), into a concrete sum over simplicial histories we still need to associate a metric and an action to each simplicial complex to be considered. Note that up to now we have not specified any kind of metric information associated with simplicial complexes. Once we have fixed the topology of the underlying simplicial complex, the most convenient way to attach metric information to it, is to use Regge calculus.

2.2 General Regge Formalism

A convenient way of defining an $n-$simplex is to specify the coordinates of its $(n+1)$ vertices, $\sigma = [0, 1, 2, ..., n]$. By specifying the squared values of the lengths of the edges $[i, j]$, s_{ij}, we fix the simplicial metric on the simplex.

$$g_{ij}(s_k) = \frac{s_{0i} + s_{0j} - s_{ij}}{2} \tag{2.2}$$

where $i, j = 1, 2, ..n$.

So if we triangulate a smooth manifold M endowed with a metric $g_{\mu\nu}$ by a homeomorphic simplicial manifold $\mathcal{M}$, the metric information is transferred to the simplicial metric of that simplicial complex

$$g_{\mu\nu}(x) \longrightarrow g_{ij}(\{s_k\}) = \frac{s_{0i} + s_{0j} - s_{ij}}{2} \tag{2.3}$$

In the continuum framework the sum over metrics is implemented through a functional integral over the metric components $\{g_{\mu\nu}(x)\}$. In the simplicial framework the metric degrees of freedom are the squared edge lengths, and so the functional integral is replaced by a simple multiple integral over the values of the edge lengths. But not all edge lengths have equal standing. Only the ones associated with the interior of the simplicial complex get to be integrated over. The boundary edge lengths remain after the sum over metrics and become the arguments of the wavefunction of the universe.

$$\int Dg_{\mu\nu}(x) \longrightarrow \int D\{s_i\} = \prod \int d\mu(s_i) \tag{2.4}$$

In the simplicial framework the fact that the geometry of the complexes is completely fixed by the specification of the squared values of all edge lengths, means that all geometrical quantities, such as volumes and curvatures, can be expressed completely in terms of those edge lengths. Consequently the Regge action (the simplicial analogue of the Einstein action

for GR) associated with a complex of known topology can be expressed exclusively in terms of those edge lengths.

The Euclideanized Einstein action for a smooth 4−manifold M with boundary ∂M, and endowed with a 4−metric, $g_{\mu\nu}$, and a scalar field Φ with mass m, is

$$\begin{aligned} I[M, g_{\mu\nu}, \phi] &= -\int_M d^4x\sqrt{g}\frac{(R-2\Lambda)}{16\pi G} - \int_{\partial M} d^3x\sqrt{h}\frac{K}{8\pi G} + \\ &+ \frac{1}{2}\int_M d^4x\sqrt{g}(\partial_\mu\phi\partial^\mu\phi + m^2\phi^2) \end{aligned}$$

where K is the extrinsic curvature.

Its simplicial analogue will be the Regge action for a combinatorial 4−manifold, $\mathcal{M}$, with squared edge lengths $\{s_k\}$, and with a scalar field taking values $\{\phi_v\}$ for each vertex v of $\mathcal{M}$, [9]:

$$\begin{aligned} I[\mathcal{M}, \{s_k\}, \{\phi_v\}] &= \frac{-2}{16\pi G}\sum_{\sigma_2^i} V_2(\sigma_2^i)\theta(\sigma_2^i) + \frac{2\Lambda}{16\pi G}\sum_{\sigma_4} V_4(\sigma_4) \\ &- \frac{2}{16\pi G}\sum_{\sigma_2^b} V_2(\sigma_2^b)\psi(\sigma_2^b) + \frac{1}{2}\sum_{\sigma_1=[ij]} \tilde{V}_4(\sigma_1)\frac{(\phi_i-\phi_j)^2}{s_{ij}} \\ &+ \frac{1}{2}\sum_j \tilde{V}_4(j)m^2\phi_j^2 \end{aligned}$$

where:

- σ_k denotes a k−simplex belonging to the set Σ_k of all k−simplices in $\mathcal{M}$.
- $\theta(\sigma_2^i)$, is the deficit angle associated with the interior 2−simplex $\sigma_2^i = [ijk]$

$$\theta(\sigma_2^i) = 2\pi - \sum_{\sigma_4 \in St(\sigma_2^i)} \theta_d(\sigma_2^i, \sigma_4) \tag{2.5}$$

  and $\theta_d(\sigma_2^i, \sigma_4)$ is the dihedral angle between the 3−simplices $\sigma_3 = [ijkl]$ and $\sigma_3^{'} = [ijkm]$, of $\sigma_4 = [ijklm]$ that intersect at σ_2^i. Its full expression is given by [5].

- $\psi(\sigma_2^b)$ is the deficit angle associated with the boundary 2−simplex σ_2^b:

$$\psi(\sigma_2^b) = \pi - \sum_{\sigma_4 \in St(\sigma_2^b)} \theta_d(\sigma_2^b, \sigma_4) \tag{2.6}$$

- $V_k(\sigma_k)$ for $k = 2, 3, 4$ is the $k-$volume associated with the $k-$simplex, σ_k, and once again their explicit expressions in terms of the squared edge lengths are given by [5].

- $\tilde{V}_4(\sigma_1)$, is the $4-$volume in the simplicial complex $\mathcal{M}$, associated with the edge σ_1, i.e., the volume of the space occupied by all points of $\mathcal{M}$ that are closer to σ_1 than to any other edge of $\mathcal{M}$. The same holds for $\tilde{V}_4(j)$ where j represents all vertices of $\mathcal{M}$.

It is easy to see that both $\tilde{V}_4(\sigma_1)$ and $\tilde{V}_4(j)$, can be expressed exclusively in terms of the edge lengths $\{s_k\}$. All these expressions remain valid if we consider smooth conifolds and their combinatorial counterparts.

So we see that any reasonable history in QG of the type $(X^4, A, g_{\mu\nu}, \Phi)$, where X^4 represents either a topological manifold or conifold endowed with a smooth structure A, metric $g_{\mu\nu}$, and in the presence of matter fields represented by Φ, has an *unique* simplicial analogue, $(\mathcal{X}^4, \{s_k\}, \{\Phi_j\})$. This allows us to recast the heuristic expression (1.1)in terms of this finite representation as:

$$\Psi[\partial\mathcal{X}, \{s_b\}, \{\phi_b\}] = \sum_{\mathcal{X}^4} \int D\{s_i\} D\{\phi_i\} e^{-I[\mathcal{X}^4, \{s_i\}, \{s_b\}, \{\phi_i\}, \{\phi_b\}]} \tag{2.7}$$

where

- $\{s_i\}$ are the squared lengths of the interior edges

- $\{s_b\}$ are the squared lengths of the boundary edges

- $\{\phi_i\}$ are the values of the field at the interior vertices

- $\{\phi_b\}$ are the values of the field at the boundary vertices

Although the functional integral over metrics has been written explicitly in terms of the edge lengths, this expression is still heuristic because we still need to specify the list of suitable simplicial complexes $\mathcal{X}^4$ we intend to sum over, the measure, and the integration contour to be used. One way to avoid the problems in defining one such list, namely the problems of algorithmic decidability and classifiability, (that have been discussed extensively in [2]) is to evaluate the sum approximately by singling out a subfamily of simplicial histories described by only a few parameters and carrying out the sum over these histories alone.

An example of this is to adopt a simplicial minisuperspace approximation. We now describe in some detail the minisuperspace model we shall consider.

3 Simplicial Minisuperspace

We shall reduce our attention to a significant subfamily of simplicial histories characterized by the following restrictions:

3.1 Topological Restrictions

We shall consider that the universe is well approximated as a simplicial cone $\mathcal{C}^4 = a * \mathcal{M}^3$ over a 3−dimensional closed combinatorial manifold $\mathcal{M}^3$, that is taken to triangulate the spatial 3−dimensional universe. Models of this kind have already been considered in [5].

The most distinctive feature of such a model is the simplifications introduced by the existence of only one interior vertex, the apex of the cone.

The consequences of this restriction are

- Note that the simplicial 4−complex, $\mathcal{C}^4$, in general will not be a combinatorial 4−manifold but a combinatorial 4−conifold, because all the vertices in $\mathcal{C}^4$ are manifold-like points, except the apex, a, whose link is $L(a) = \mathcal{M}^3$, and in general $\mathcal{M}^3$ will not be a combinatorial 3−sphere.

- The fact that $\mathcal{M}^3$ is closed means that the only boundary of $\mathcal{C}^4$ will be the $\mathcal{M}^3$ itself:

$$\partial\mathcal{C}^4 = \mathcal{M}^3 \tag{3.1}$$

  So the combinatorial 3−manifold $\mathcal{M}^3$ is to be seen as a triangulation of the spatial $3 - D$ universe.

- The cone structure of the $\mathcal{C}^4$ reflected in the fact that there is only one interior vertex (the apex a) means that all vertices in $\mathcal{M}^3$ will be boundary vertices of $\mathcal{C}^4$. So if $N_p(\mathcal{K}^n)$ is the number of p−simplices in the complex $\mathcal{K}^n$ we see that since $\mathcal{C}^4 = a * \mathcal{M}^3$, then

$$N_0(\mathcal{C}^4) = N_0(\mathcal{M}^3) + 1 \tag{3.2}$$

  And in general there will be two kinds of p−simplices ($p = 1, 2, 3$), in $\mathcal{C}^4$, the ones that exist originally in $\mathcal{M}^3$, which will be the boundary p−simplices of $\mathcal{C}^4$, and the p−simplices generated as cones over the $(p-1)$−simplices of $\mathcal{M}^3$ with apex a. These will be the interior p−simplices of $\mathcal{C}^4$. So in general

$$\sigma_p^{bound}(\mathcal{C}^4) = \sigma_p(\mathcal{M}^3)$$
$$\sigma_p^{inter}(\mathcal{C}^4) = a * \sigma_{p-1}(\mathcal{M}^3)$$

and

$$N_0(\mathcal{C}^4) = N_0(\mathcal{M}^3) + 1$$
$$N_1(\mathcal{C}^4) = N_1(\mathcal{M}^3) + N_0(\mathcal{M}^3)$$
$$N_2(\mathcal{C}^4) = N_2(\mathcal{M}^3) + N_1(\mathcal{M}^3)$$
$$N_3(\mathcal{C}^4) = N_3(\mathcal{M}^3) + N_2(\mathcal{M}^3)$$
$$N_4(\mathcal{C}^4) = N_3(\mathcal{M}^3)$$

- The Euler characteristic of a simplicial complex $\mathcal{K}^n$ is

$$\chi(\mathcal{K}^n) = N_0(\mathcal{K}^n) - N_1(\mathcal{K}^n) + N_2(\mathcal{K}^n) - N_3(\mathcal{K}^n)... \pm N_n(\mathcal{K}^n)$$

  with $+$ if n is even and $-$ if n is odd. On the other hand, since $\mathcal{M}^3$ is a closed combinatorial manifold, then its Euler characteristic must vanish, and so we have

$$N_0(\mathcal{M}^3) - N_1(\mathcal{M}^3) + N_2(\mathcal{M}^3) - N_3(\mathcal{M}^3) = 0 \tag{3.3}$$

- Since $\mathcal{M}^3$ is a closed, pure, non branching complex then all its $2-$simplices must belong to exactly two $3-$simplices of $\mathcal{M}^3$

$$N_2(\mathcal{M}^3) = 2N_3(\mathcal{M}^3) \tag{3.4}$$

In the table below we list the values of N_0, and N_3 for some of the most relevant closed connected combinatorial $3-$manifolds $\mathcal{M}^3$

$\mathcal{M}^3$	N_0	N_3	$S_{crit}^{m=0}$
α_4	5	5	29.31
$\mathcal{S}^2 \times \mathcal{S}^1$	10	30	5.61
$\mathcal{L}(2,1)$	11	30	3.54
$\mathcal{L}(5,1)$	15	89	-0.84
$\mathcal{T}^3$	15	90	-0.31

where

- α_4 is the simplest triangulation of S^3, [4].
- $\mathcal{S}^2 \times \mathcal{S}^1$ and $\mathcal{T}^3$ are simple triangulations of the spaces $S^2 * S^1$ and T^3 constructed in [11].
- $\mathcal{L}(p,1)$ are simple triangulations of their respective Lens spaces, $L(p,1)$ used in [5].

The meaning and relevance of the values in the last column will be explained later.

3.2 Metric Restrictions

Up to now we have concentrated on the restrictions on the topology of the simplicial space-times that characterize our minisuperspace models. The restrictions on the metric degrees of freedom are as important.

By assuming a cone-like structure $\mathcal{C}^4 = a * \mathcal{M}^3$, we see that all the interior edges of $\mathcal{C}^4$ are of the same type ,i.e., one of the vertices is a boundary vertex belonging to $\mathcal{M}^3$, and the other is the (single) interior vertex of $\mathcal{C}^4$, its apex.

If we label the interior vertex as 0 and the other (boundary) vertices of $\mathcal{C}^4$ as $1, 2, ...,$-$N_0(\mathcal{M}^3)$. Then the cone-like structure of $\mathcal{C}^4$ leads to all interior edges being of the same form $[0, \alpha]$, with $\alpha = 1, 2, .., N_0(\mathcal{M}^3)$.

So it makes sense to introduce the restriction that all interior edges have equal lengths whose squared value is denoted $s_i = s_{0\alpha}$. A similar assumption is made with respect to the boundary edge lengths, i.e., we consider them all to be equal to a common value $s_{ij} = s_b$, with $i, j = 1, 2, .., N_0(\mathcal{M}^3)$.

We are well aware that these simplifications greatly reduce the scope of the model, namely because they result in there being only one kind of $4-$simplex in the complex. Thus any real classical solution will necessarily be either purely Lorentzian or Euclidean. However,

it is well known that in the analogous continuum minisuperspace model, complex classical solutions not only exist but in the late Universe even dominate the path integral, [10]. In order to begin to circumvent this problem we are currently studying a similar model with two different interior edge lengths.

3.3 Scalar Field

The simplifications assumed in respect to the edge lengths makes it natural to assume that the scalar field is spatially homogeneous. So we assume that the scalar field takes the same value ϕ_b for all boundary vertices of $\mathcal{C}^4$. The value at the interior vertex, ϕ_i, is independent.

3.4 Minisuperspace Wavefunction

We can now concretely implement a simplicial minisuperspace approximation to the wavefunction of the universe of the type (2.7), as

$$\Psi[\mathcal{M}^3, s_b, \phi_b] = \int ds_i d\phi_i e^{-I[a*\mathcal{M}^3, s_i, s_b, \phi_i, \phi_b]} \tag{3.5}$$

The Regge action for this minisuperspace can now be calculated. For simplicity we introduce rescaled metric variables:

$$\xi = \frac{s_i}{s_b} \tag{3.6}$$

$$S = \frac{H^2 s_b}{l^2} \tag{3.7}$$

where $H^2 = l^2\Lambda/3$, and $l^2 = 16\pi G$ is the Planck length. We shall work in units where $c = \hbar = 1$.

Then the volume of the 4−simplices in $\mathcal{C}^4$ is

$$V_4(\sigma_4) = \frac{l^4}{24\sqrt{2}H^4} S^2 \sqrt{\xi - 3/8} \tag{3.8}$$

The volume of the $N_1(\mathcal{M}^3)$ internal 2−simplices, σ_2^i in $\mathcal{C}^4$ is

$$V_2(\sigma_2^i) = \frac{l^2}{2H^2} S \sqrt{\xi - 1/4} \tag{3.9}$$

The volume of the $2N_3(\mathcal{M}^3)$ boundary 2−simplices, σ_2^b in $\mathcal{C}^4$ is

$$V_2(\sigma_2^b) = \frac{\sqrt{3}l^2}{4H^2} S \tag{3.10}$$

The volumes of the internal and boundary 3−simplices of $\mathcal{C}^4$ are, respectively

$$V_3(\sigma_3^i) = \frac{l^3}{12H^3} S^{3/2} \sqrt{3\xi - 1} \tag{3.11}$$

$$V_3(\sigma_3^b) = \frac{\sqrt{2} l^3}{12H^3} S^{3/2} \tag{3.12}$$

and so the dihedral angle associated with each internal 2−simplex is

$$\theta(\sigma_2^i) = \arccos \frac{2\xi - 1}{6\xi - 2}; \tag{3.13}$$

for the boundary 2−simplices we have

$$\theta(\sigma_2^b) = \arccos \frac{1}{2\sqrt{6\xi - 2}}. \tag{3.14}$$

With respect to the matter terms, the kinetic term vanishes when the edges σ_2 are boundary edges. The only non vanishing contribution comes from the internal edges $\sigma_2 = [0j]$.

Computing the relevant volumes associated with the internal edges and all the vertices it is possible to conclude that the Regge action for this simplicial minisuperspace is

$$\begin{aligned} I[\xi, S, \phi_i, \phi_b] &= -\frac{S}{H^2}\Big\{(N_3\sqrt{3})\Big[\pi - 2\arccos\frac{1}{2\sqrt{6\xi-2}}\Big] \\ &+ N_1\sqrt{\xi - 1/4}\Big[2\pi - \frac{6N_3}{N_1}\arccos\frac{2\xi-1}{6\xi-2}\Big] \\ &- \Big(\frac{N_3}{120\sqrt{2}}\Big)\frac{\sqrt{\xi-3/8}}{\xi}(\phi_i l - \phi_b l)^2\Big\} + \frac{S^2}{H^2}\Big\{\Big(\frac{N_3}{4\sqrt{2}}\Big)\sqrt{\xi-3/8} \\ &+ \frac{N_3}{240\sqrt{2}}\Big(\frac{m^2l^2}{H^2}\Big)\sqrt{\xi-3/8}(\phi_i^2 l^2 + 4\phi_b^2 l^2)\Big\} \end{aligned} \tag{3.15}$$

where N_0, N_1 and N_3 all refer to $\mathcal{M}^3$.

We see that the dependence of the action on the topology of the underlying $\mathcal{M}^3$ is contained in the parameters N_0 and N_3, $(N_1 = N_0 + N_3)$. The metric dependence is obviously contained in ξ and S, and its dependence on the matter field in ϕ_i and ϕ_b.

Note that the previous expressions are valid for a wide variety of simplicial geometries with very different spatial topologies (of $\mathcal{M}_3$). Different triangulations of the $3-D$ spatial universe have different values of N_0 and N_3 and consequently different actions. But as long

as they are closed connected combinatorial manifolds the previous expressions hold and so the functional dependence of the action on s_i and s_b remains the same.

So given a certain underlying simplicial complex $a * \mathcal{M}^3$ (with fixed N_0 and N_3) we see that in order to approximate the heuristic expression (1.1) by a fully computable expression

$$\Psi[\mathcal{M}^3; s_b; \phi_b] = \Psi[N_0, N_3; S; \phi_b] = \int_C D\xi D\phi_i e^{-I[N_0,N_3;S,\xi;\phi_b,\phi_i]} \tag{3.16}$$

we only need to specify the integration contour C, and the measure of integration $D\xi D\phi_i$.

In our simplified models the result yielded by a contour C is not very sensitive to the choice of measure if we stick to the usual measures, i.e., polynomials of the squared edge lengths. In our case we take

$$D\xi D\phi_i = \frac{ds_i}{2\pi i l^2} d\phi_i = \frac{S}{2\pi i H^2} d\xi d\phi_i \tag{3.17}$$

In the search for the correct integration contour for our simplicial minisuperspace model we start by reviewing some of the main results for the general continuum case.

Unfortunately, in the case of closed cosmologies there is as yet no known explicit prescription for the integration contour. So usually one takes a pragmatic view, in which we look for contours that lead to the desired features of the wavefunction of the universe. Following [12], these features are:

- It should yield a convergent path integral
- The resulting wavefunction should predict classical spacetime in the late universe, i.e, oscillating behaviour when the Ψ is well approximated by the semiclassical approximation.
- The resulting wavefunction should obey the diffeomorphism constraints, in particular the Wheeler-DeWitt equation.

It is well known that any integration contour over real metrics would yield a wavefunction that does not satisfy any of these basic requirements. On the other hand, an integration contour over complex metrics can, if wisely chosen, lead to a wavefunction that satisfies those requirements.

In the simplicial framework, complex metrics arise from complex-valued squared edge lengths, (2.2). The boundary squared edge length, S, has to be real and positive for obvious

physical reasons. But the interior squared edge length, ξ, can be allowed to take complex values. Before we attempt to choose the correct integration contour it is essential we study the analytical and asymptotic properties of the action as a function of the complex variable ξ.

3.5 Analytic Study of the Action

By allowing ξ to be complex-valued we have to contend with a multivalued Regge action, (3.15). The deficit angle terms have an infinite number of branches, and we must deal with this multivaluedness, if we are to study the behaviour of steepest descents contours,(along which the imaginary part of the action must remain constant). Furthermore, in order to obtain a continuous and single-valued action, a careful analysis of all the action's branching points is necessary. As expected these branching points occur at the values of ξ for which the simplices become degenerate, i.e, where their volumes vanish. The analytic study of the action should then enable us to obtain integration contours that avoid such branching points, and along which the action is continuous and single-valued, leading to a well defined wavefunction of the Universe.

The action (3.15) is trivially analytic with respect to the variables ϕ_i, ϕ_b and S. But its dependence on the complex-valued ξ is much more complicated. So we shall investigate the analytic properties of I as if it was a function of ξ only, $I = I[\xi]$, the other variables acting as parameters.

The function $I[\xi]$ has singularities at $\xi = 0$ and $\xi = 1/3$, and square root branch points at $\xi = 1/4$, $1/3$ and $3/8$. These branch points correspond respectively to the vanishing of the volume of the internal $2-$simplices, $3-$simplices and $4-$simplices. Using

$$\arccos z = -i \log(z + \sqrt{z^2 - 1})$$

we see that $\xi = 1/3$ is also a logarithmic branch point, near which the action behaves like :

$$I \sim i2\sqrt{3}N_3\Big(\frac{S}{H^2}\Big) \log(3\xi - 1) \tag{3.18}$$

The multivaluedness of $I[\xi]$ associated with these branch points forces us to implement branch cuts in order to obtain a continuous function. In general, for terms of the type $\sqrt{z - z_0}$ we consider a branch cut $(-\infty, z_0]$. So the branch cuts associated with the terms

$\sqrt{\xi - 3/8}$, $\sqrt{\xi - 1/4}$ and $\sqrt{\xi - 1/3}$, altogether lead to a branch cut $(-\infty, 3/8]$. On the other hand, terms of the type $\arccos(z)$ have branch points at $z = -1, +1, \infty$, and usually the associated branch cuts are chosen as $(-\infty, -1] \cup [1, +\infty)$. These terms are also infinitely multivalued.

The corresponding cuts for the term $\arccos \frac{2\xi - 1}{6\xi - 2}$ are $(\frac{1}{3}, \frac{3}{8}] \cup [\frac{1}{4}, \frac{1}{3})$. On the other hand, associated with the term $\arccos \frac{1}{2\sqrt{6\xi - 2}}$ we have one cut $(\frac{1}{3}, \frac{3}{8}]$ associated with $\arccos u(z)$, and another $(-\infty, \frac{1}{3}]$ associated with $u(z) = \sqrt{6\xi - 2}$.

So when we consider all these branch cuts simultaneously, we see that one way to obtain a continuous action I as a function of ξ, is to consider a total branch cut $(-\infty, \frac{3}{8}]$. Note that this also takes care of the singularity at $\xi = 0$

Although the action then becomes a continuous function of ξ in the complex plane with a cut $(-\infty, \frac{3}{8}]$, it is still infinitely multivalued. As usual in similar cases in order to remove this multivaluedness we redefine the domain where the action is defined, from the complex plane to the Riemann surface associated with I. The infinite multivaluedness of the action reflects itself in I having an infinite number of branches with different values. The Riemann surface is composed of an infinite number of identical sheets, $\mathbb{C} - (-\infty, \frac{3}{8}]$, one sheet for each branch of I.

We define the first sheet $\mathbb{C}_1$ of $I[\xi]$ as the sheet where the terms in $\arccos(z)$ assume their principal values. So the action in the first sheet will be formally equal to the original expression (3.15), with positive signs taken for the square root factors. Note that with the first sheet defined in this way, for real $\xi > 3/8$ the volumes and deficit angles are all real, leading to a real Euclidean action for $\xi \in [\frac{3}{8}, +\infty)$ on the first sheet. On the other hand, when ξ is real and less than $1/4$ in the first sheet , the volumes become pure imaginary and the Euclidean action becomes pure imaginary. For all other points of this first sheet the action is fully complex.

Since by (2.2) we see that the simplicial metric in each $4-$simplex is real iff ξ is real, then the simplicial geometries built out of these $4-$simplices will be real when ξ is real. Furthermore the corresponding eigenvalues of g_{ij} are $\lambda = \{4(\xi - 3/8), 1/2, 1/2, 1/2\}$, [5]. So we see that for real $\xi > 3/8$ we have real Euclidean signature geometries, with real Euclidean action, and for real $\xi < 1/4$, we have real Lorentzian signature geometries with pure imaginary Euclidean action.

Up to now we have been concerned with what happens in the first sheet only. When we continue the action in ξ around one or more branch points, we will leave this first sheet and

emerge in some other sheet of the Riemann surface. Only a few of these other sheets are relevant to us.

When the action is continued in ξ once around all finite branch points ($\xi = 1/4, 1/3, 3/8$), we reach what shall be called the second sheet . It is easy to conclude that the action in this second sheet is just the negative of the action in the first sheet.

$$I^I[\xi, S, \phi_i, \phi_b] = -I^{II}[\xi, S, \phi_i, \phi_b] \tag{3.19}$$

Once in the second sheet, if we encircle the branch points in such a way that we cross the branch cut, $(-\infty, \frac{3}{8}]$, between 1/4 and 1/3, we arrive at what we shall call the third sheet. By doing this the terms $\pi - 2\arccos\frac{1}{2\sqrt{6\xi-2}}$ and $\arccos\frac{2\xi-1}{6\xi-2}$, both flip signs and so the action in this third sheet is

$$\begin{aligned} I^{III}[\xi, S, \phi_i, \phi_b] &= -\frac{S}{H^2}\Big\{\Big(N_3\sqrt{3}\Big)\Big[\pi - 2\arccos\frac{1}{2\sqrt{6\xi-2}}\Big] \\ &- N_1\sqrt{\xi - 1/4}\Big[2\pi + \frac{6N_3}{N_1}\arccos\frac{2\xi-1}{6\xi-2}\Big] \\ &- \Big(\frac{N_3}{120\sqrt{2}}\Big)\frac{\sqrt{\xi-3/8}}{\xi}(\phi_i l - \phi_b l)^2\Big\} + \frac{S^2}{H^2}\Big\{\Big(\frac{N_3}{4\sqrt{2}}\Big)\sqrt{\xi-3/8} \\ &+ \frac{N_3}{240\sqrt{2}}\Big(\frac{m^2l^2}{H^2}\Big)\sqrt{\xi-3/8}(\phi_i^2 l^2 + 4\phi_b^2 l^2)\Big\} \end{aligned}$$

If instead of crossing the cut between 1/4 and 1/3, we transverse it between 1/3 and 3/8 then we will end up in a different sheet. However, the asymptotic behaviour of the action is similar to that on the third sheet, so we will not go into the details.

3.6 Asymptotic Behaviour of the Action

In any investigation of the correct contour of integration it is essential to know how the action behaves asymptotically with respect to the variable ξ, ($\xi \to \infty$), because only then will we be able to evaluate the contribution coming from these regions.

In the first sheet when $\xi \to \infty$ the action behaves like

$$I^I[\xi, S, \phi_i, \phi_b] \sim \frac{\frac{N_3}{4\sqrt{2}} + A(\phi_i, \phi_b)}{H^2} S(S - S_{crit})\sqrt{\xi} \tag{3.20}$$

where

$$A(\phi_i, \phi_b) = \frac{1}{240\sqrt{2}} \frac{m^2 l^2}{H^2} N_3 (\phi_i^2 l^2 + 4\phi_b^2 l^2) \tag{3.21}$$

and

$$S_{crit} = \frac{N_1[2\pi - \frac{6N_3}{N_1} \arccos(1/3)]}{\frac{N_3}{4\sqrt{2}} + A(\phi_i, \phi_b)} \tag{3.22}$$

The asymptotic behaviour of I^I for large ξ depends on whether or not S is larger than the critical value S_{crit}. This value will also be crucial for the classical solutions to be obtained in the next section.

First note that there are two important special cases:

- The pure gravity model, $m = 0, \phi = 0$, in which we are reduced to the kind of models considered in [5].
- The massless scalar field model, $m = 0$.

In both cases $A(\phi_i, \phi_b) = 0$, and the asymptotic behaviour becomes independent of the matter field sector. In both cases as $\xi \to \infty$ we have:

$$I^{I\, m=0}[\xi, S, \phi_i, \phi_b] \sim \frac{N_3}{4\sqrt{2}} \frac{1}{H^2} S(S - S_{crit}^{m=0}) \sqrt{\xi} \tag{3.23}$$

where

$$S_{crit}^{m=0} = \frac{4\sqrt{2} N_1}{N_3} \Big[2\pi - \frac{6N_3}{N_1} \arccos(1/3) \Big] \tag{3.24}$$

Note that once $A(\phi_i, \phi_b) \geq 0$, then $S_{crit}^{m=0} \geq S_{crit}$.

For the second sheet obviously the asymptotic behaviour of the action is just the negative of that in the first sheet. For the third sheet the situation is slightly different because only some terms in the action change sign and we have that as $\xi \to \infty$:

$$I^{III}[\xi, S, \phi_i, \phi_b] \sim \frac{\frac{N_3}{4\sqrt{2}} + A(\phi_i, \phi_b)}{H^2} S(S + S_{crit}^{III}) \sqrt{\xi} \tag{3.25}$$

where

$$S_{crit}^{III} = \frac{N_1[2\pi + \frac{6N_3}{N_1} \arccos(1/3)]}{\frac{N_3}{4\sqrt{2}} + A(\phi_i, \phi_b)} \tag{3.26}$$

As before we consider the two sub-cases where $A(\phi_i, \phi_b) = 0$

$$I^{III\,m=0}[\xi, S, \phi_i, \phi_b] \sim \frac{N_3}{4\sqrt{2}} \frac{1}{H^2} S(S + S^{III m=0}_{crit})\sqrt{\xi} \tag{3.27}$$

and

$$S^{III m=0}_{crit} = \frac{4\sqrt{2}N_1}{N_3}\Big[2\pi + \frac{6N_3}{N_1}\arccos(1/3)\Big] \tag{3.28}$$

4 Classical Solutions

The classical simplicial geometries are the extrema of the Regge action we have obtained above. In our minisuperspace model there are two degrees of freedom ξ, ϕ_i. So the Regge equations of motion will be:

$$\frac{\partial I}{\partial \xi} = 0 \tag{4.1}$$

and

$$\frac{\partial I}{\partial \phi_i} = 0 \tag{4.2}$$

They are to be solved for the values of ξ, ϕ_i, subject to the fixed boundary data S, ϕ_b. The classical solutions will thus be of the form $\overline{\xi}(S, \phi_b)$, and $\overline{\phi}_i(S, \phi_b)$. The solution $\overline{\xi}(S, \phi_b)$ completely determines the simplicial geometry. For the general model equations(4.1), (4.2), take the form

$$S = \frac{\frac{a_1}{2}\frac{1}{\sqrt{\xi - 1/4}}[2\pi - a_2 \arccos\frac{2\xi-1}{6\xi-2}] + \frac{N_3}{240\sqrt{2}}\frac{\xi - 3/4}{\xi^2\sqrt{\xi - 3/8}}(\phi_i - \phi_b)^2 l^2}{\frac{a_3}{2\sqrt{\xi - 3/8}} + \frac{1}{480\sqrt{2}}(\frac{m^2 l^2}{H^2})\frac{N_3}{\sqrt{\xi - 3/8}}(\phi_i^2 l^2 + 4\phi_b^2 l^2)} \tag{4.3}$$

and

$$\phi_i = \frac{\phi_b}{1 + \frac{1}{2}\frac{m^2 l^2}{H^2}\xi S} \tag{4.4}$$

Note that we will be expressing the values of the field ϕ and its mass m, in Planck units (l^{-1}). Furthermore, for simplicity of notation we have introduced $a_1 = N_1$, $a_2 = 6N_3/N_1$ and $a_3 = N_3/(4\sqrt{2})$.

Note that these expressions were obtained using the expression for the action on the first sheet. Of course, since on the second sheet the action is just the negative of this, the equations of motion are the same. And obviously every classical solution $\overline{\xi}_I(S, \phi_b)$ located

on the first sheet will have a counterpart $\overline{\xi}_{II}$ of the same numerical value, but located on the second sheet, and so with an action of opposite sign, $I[\overline{\xi}_I(S,\phi_b)] = -I[\overline{\xi}_{II}(S,\phi_b)]$. So the classical solutions occur in pairs.

For physical reasons the squared boundary edge length, S, has to be real and positive, and we will also assume that ϕ_b is real.

Before we go on to study the general model it is useful to investigate the two special cases mentioned in section **3.6**, i.e., pure gravity, and massless scalar field.

4.1 Pure Gravity

In this case our model is reduced to a family of models already considered by [5], where we have only one metric degree of freedom ξ and its associated equation of motion is

$$S = \frac{a_1}{a_3}\sqrt{\frac{\xi - 3/8}{\xi - 1/4}}\Big[2\pi - a_2 \arccos\frac{2\xi - 1}{6\xi - 2}\Big] \tag{4.5}$$

The condition of real positive S means that physically acceptable classical solutions occur only for real $\xi > 3/8$ and real $\xi < 1/4$. There are two different kinds of classical solutions according to whether $S^{m=0}_{crit}$ is negative or positive.

For positive $S^{m=0}_{crit}$ the general form of the solutions is similar to that of the $\mathcal{S}^2 \times \mathcal{S}^1$ model in Figure 1.There are two different regimes: For every S between 0 and S_{crit}, the classical solutions $\overline{\xi}_I(S) = \overline{\xi}_{II}(S)$ are real and belong to $[3/8, +\infty)$. So they correspond to Euclidean signature simplicial geometries and their Euclidean actions will be real (but symmetric). For every $S > S_{crit}$ the classical solutions $\overline{\xi}_I(S) = \overline{\xi}_{II}(S)$ are real and belong to $(-\infty, 1/4]$. So they correspond to Lorentzian signature simplicial geometries and their Euclidean actions are pure imaginary

$$I[\overline{\xi}_I(S)] = -I[\overline{\xi}_{II}(S)] = i\tilde{I}[\overline{\xi}_I(S)] \tag{4.6}$$

where $\tilde{I}[\overline{\xi}_I(S)]$ is real.

When S_{crit} is negative there is no Euclidean regime. All classical solutions are Lorentzian geometries. For each $S > 0$, there is a pair of solutions $\overline{\xi}_I(S) = \overline{\xi}_{II}(S) \in (-\infty, 1/4]$ on the first and second sheets. Their corresponding actions are pure imaginary, as in (4.6).

4.2 Massless Scalar Field

In this case, as in the general model there are two degrees of freedom ξ and ϕ_i. The corresponding equations of motion are

$$S = \frac{a_1}{a_3}\sqrt{\frac{\xi - 3/8}{\xi - 1/4}}\Big[2\pi - a_2 \arccos\frac{2\xi - 1}{6\xi - 2}\Big] + \frac{N_3}{120\sqrt{2}a_3}\frac{1}{\xi}\Big(1 - \frac{3}{4\xi}\Big)(\phi_i - \phi_b)^2 \tag{4.7}$$

and

$$\phi_i = \phi_b \tag{4.8}$$

If we substitute the second equation into the first we see that it reduces to the equation for ξ of the previous case. So the classical solutions for ξ in the massless case coincide with the pure gravity case, $\overline{\xi}(S, \overline{\phi}_i = \phi_b) = \overline{\xi}(S)$. So the presence of the massless scalar field does not change the simplicial geometries that are classical solutions. Furthermore, the actions associated with these classical solutions are independent of the scalar field and coincide with the actions associated with the previous model.

$$I[\overline{\xi}, \overline{\phi}_i = \phi_b] = I[\overline{\xi}] \tag{4.9}$$

4.3 Massive Scalar Field

Given the classical equations of motion (4.3) and (4.4), introducing the second equation into the first yields a cubic equation on S for each value of ξ, given fixed ϕ_b. That equation is

$$A_3(\xi)S^3 + A_2(\xi)S^2 + A_1(\xi)S + A_0(\xi) = 0 \tag{4.10}$$

where

$$A_3(\xi) = \frac{a_3}{2}\Big[K^2 + \frac{2}{15}K^3\phi_b^2\Big]\xi^2 \tag{4.11}$$

$$\begin{aligned} A_2(\xi) &= a_3\Big[K + \frac{2}{15}K^2\phi_b^2\Big]\xi - \frac{a_1}{2}K^2\xi^2\sqrt{\frac{\xi - 3/8}{\xi - 1/4}}\Big[2\pi - a_2 \arccos\frac{2\xi - 1}{6\xi - 2}\Big] \\ &- \frac{a_3}{60}K^2\phi_b^2(\xi - 3/4) \end{aligned}$$

$$A_1(\xi) = \frac{a_3}{2}\Big(1 + \frac{K\phi_b^2}{6}\Big) - a_1 K\xi\sqrt{\frac{\xi - 3/8}{\xi - 1/4}}\Big[2\pi - a_2 \arccos\frac{2\xi - 1}{6\xi - 2}\Big] \tag{4.12}$$

$$A_0 = -\frac{a_1}{2}\sqrt{\frac{\xi - 3/8}{\xi - 1/4}}[2\pi - a_2 \arccos\frac{2\xi - 1}{6\xi - 2}] \tag{4.13}$$

where $K = (1/2)(ml/H)^2$.

The more complicated dependence on ξ leads us to solve the classical equation in order to find S for each value of ξ. By inverting the resulting solutions we obtain $\overline{\xi}(S, \phi_b)$, and consequently $\overline{\phi}_i(S, \phi_b)$, via (4.4). This being a cubic equation we expect 3 solutions for each value of ξ. However, because of obvious physical constraints we will accept only solutions that are real and positive.

Of course as in the pure gravity model, classical solutions occur in pairs, one on the first sheet and the other on the second sheet. They have the same numerical value but yield actions of opposite sign.

Instead of presenting $\overline{\xi} = \overline{\xi}(S, \phi_b)$ as a 3−D plot it is more informative to consider the graphs of $\overline{\xi} = \overline{\xi}(S)$ for several values of ϕ_b. Figure 2 shows one such plot for a cone over the α_4 triangulation of the 3−sphere, in the presence of a scalar field of mass $m = 1(l^{-1})$, and a boundary value $\phi_b = 1(l^{-1})$.

Note that near $\xi = 1/4$ the solution is similar to a solution in the pure gravity model. This is to be expected because around $\xi = 1/4$ the curvature (Ricci scalar) term dominates all others, including the matter terms in the action. So for large values of S, that is, for $\xi \to \frac{1}{4}^-$, the classical solutions in the massive scalar field model will be well approximated by their analogues in the pure gravity model.

Away from the singularity the situation is different. In the Euclidean regime, $\xi > 3/8$, there is always only one real positive solution of (4.10) for each value of ξ. Furthermore, as $\xi \to +\infty$, S converges to a critical value dependent on the value of the mass m and boundary value of the scalar field ϕ_b:

$$S^m_{crit} = \frac{a_1}{a_3}\Big[2\pi - a_2 \arccos(1/3)\Big]\Big(\frac{1}{1 + \frac{2}{15}K\phi_b^2}\Big) = S^{m=0}_{crit} \times \Big(\frac{1}{1 + \frac{2}{15}K\phi_b^2}\Big) \tag{4.14}$$

This way the effective critical value decreases as the values of m or ϕ_b increase.

In the Lorentzian regime, $\xi < 1/4$, the presence of matter radically changes the classical solutions. When ξ is sufficiently negative, i.e., $\xi < \xi_0$, there are 3 real positive solutions of

(4.10) for each value of ξ. One of these branches is almost constant and rapidly converges to S_{crit} as ξ decreases. Another branch also starts at ξ_0, but then converges to zero as $\xi \to -\infty$. Finally, the third branch, which also converges to zero as $\xi \to -\infty$, but continues all the way to $\xi = 1/4$, where $S \to +\infty$. It is this last branch of classical solutions that is relevant to us, because it is the only one that continues beyond S_{crit} all the way to $S \to +\infty$.

So for $S \in [0, S_{crit})$, we will have:

- Two pairs of real Lorentzian signature solutions $\overline{\xi}_I^{L1}(S, \phi_b) = \overline{\xi}_{II}^{L1}(S, \phi_b) \in (-\infty, 1/4]$, and $\overline{\xi}_I^{L2}(S, \phi_b) = \overline{\xi}_{II}^{L2}(S, \phi_b) \in (-\infty, 1/4]$ with pure imaginary Euclidean actions.
- One pair of real Euclidean signature solutions $\overline{\xi}_I^{E}(S, \phi_b) = \overline{\xi}_{II}^{E}(S, \phi_b) \in [3/8, +\infty)$, with real Euclidean action.

For $S > S_{crit}$, we will have:

- Only one pair of real solutions $\overline{\xi}_I(S, \phi_b) = \overline{\xi}_{II}(S, \phi_b) \in (-\infty, 1/4]$ that correspond to Lorentzian signature simplicial metrics, and whose Euclidean actions, though symmetric, are both pure imaginary.

$$I[\overline{\xi}_I(S, \phi_b)] = -I[\overline{\xi}_{II}(S, \phi_b)] = i\tilde{I}[\overline{\xi}_I(S, \phi_b)]$$

If we increase the value of m or ϕ_b, the value of S_{crit} decreases to zero and eventually the branch associated with the Euclidean regime vanishes. The same happens to the two extra Lorentzian branches that are contained in $[0, S_{crit})$, and we are left with a situation similar to the one we found in the pure gravity model when $S_{crit}^{m=0}$ becomes < 0. That is, there remains only one Lorentzian branch for the entire range of S, from $S = 0$ to $S \to +\infty$. For other topologies like $\mathcal{T}^3$ there is no Euclidean regime whatever the value of the field, because $S_{crit} < S_{crit}^{m=0} < 0$. See Figure 3.

5 Semiclassical Approximation

One of the main requirements on any model is that it yields a wavefunction that in the late universe predicts a classical (Lorentzian) spacetime, like the one we experience. Now, a wavefunction of the universe will predict a classical spacetime where it is well approximated by the semiclassical approximation associated with Lorentzian classical solutions. We shall

see what are the conditions that lead to such a situation in the next section. For now we will assume that this is the case and concentrate on the semiclassical approximation.

The semiclassical wavefunction for our model will be obtained from the full wavefunction

$$\Psi(S,\phi_b) = \frac{S}{2\pi i H^2}\int_C d\xi d\phi_i e^{-I(\xi,S,\phi_i,\phi_b)} \tag{5.1}$$

by assuming that the integral is dominated by the contributions of the stationary points of the Regge action, i.e., the classical solutions computed above.

We shall consider that the first integration is over the complex valued ξ and then over the real valued ϕ_b. We then assume that for each pair of boundary data (S,ϕ_b), the integral over ξ is dominated by the contributions coming from the classical solutions $\{\overline{\xi}_k(S,\phi_b)\}$. If these are real Lorentzian solutions with purely imaginary actions $I_k = i\tilde{I}[\overline{\xi}_k(S,\phi_b);\phi_i] = i\tilde{I}_k(S,\phi_b,\phi_i)$, then the semiclassical approximation for the integral over ξ is

$$\int_C d\xi e^{-I(\xi,S,\phi_i,\phi_b)} \sim \sum_k \sqrt{\frac{S^2}{2\pi H^4 \mid \tilde{I}''[\overline{\xi}_k(S,\phi_b),\phi_i] \mid}} e^{-i[\tilde{I}(\overline{\xi}_k(S,\phi_b),\phi_i)+\mu_k\frac{\pi}{4}]} \tag{5.2}$$

where $'$ means derivative with respect to ξ and $\mu_k = sgn(\tilde{I}'')$.

The remaining integrals over ϕ_i are now Fourier-type integrals, and can be evaluated by the stationary phase method by the contribution coming from their stationary points which are precisely the classical solutions $\overline{\phi}_i^k(S,\phi_b)$

$$\begin{aligned}\Psi_{SC}(S,\phi_b) &\sim \int d\phi_i \sum_k \sqrt{\frac{S^2}{2\pi H^4 \mid \tilde{I}''[\overline{\xi}_k(S,\phi_b),\phi_i] \mid}} e^{-i[\tilde{I}(\overline{\xi}_k(S,\phi_b),\phi_i)+\mu_k\frac{\pi}{4}]} \\ &\sim \sum_k \sqrt{\frac{S^2}{2\pi H^4 \mid \tilde{I}_k''(S,\phi_b) \mid}} e^{-i[\tilde{I}_k(S,\phi_b)+\mu_k\frac{\pi}{4}]}\end{aligned}$$

where $I_k(S,\phi_b) = I[\overline{\xi}_k(S,\phi_b),\overline{\phi}_i^k(S,\phi_b)]$.

When the dominant extrema are real Euclidean solutions $\{\overline{\xi}_k(S,\phi_b)\}$, with real Euclidean actions $I_k(S,\phi_b)$ then the semiclassical evaluation of the integral over ξ leads to Laplace-type integrals over ϕ_i which once more are dominated by the contributions coming from the stationary points of $I[\overline{\xi}_k(S,\phi_b),\phi_i]$, which are precisely the classical solutions $\overline{\phi}_i^k(S,\phi_b)$. So the semiclassical wavefunction will then be

$$\Psi_{SC}(S,\phi_b) \sim \sum_k \sqrt{\frac{S^2}{2\pi H^4 \mid I_k''(S,\phi_b) \mid}} e^{-I_k(S,\phi_b)} \tag{5.3}$$

We shall be mainly interested in the behaviour of the wavefunction of the universe for large S, (relative to Planck's length, l) because that corresponds to the late universe we experience.

The semiclassical approximations associated with pure gravity models were calculated in [4] and [5] . In these models when S is large, the only classical solutions are a pair of real Lorentzian geometries, $\overline{\xi}_I(S) = \overline{\xi}_{II}(S) \in (-\infty, 1/4]$, with purely imaginary Euclidean actions, and so the semiclassical approximation associated with them yields an oscillating wavefunction for $S > S_{crit}$, as desired.

For the massless scalar field model the classical solutions have the same simplicial geometry, as in pure gravity case, since $\overline{\phi_i} = \phi_b$, implies that $\overline{\xi}_k(S, \phi_b) = \overline{\xi}_k(S)$, where $k = I, II$. So the action associated with the classical solutions is independent of ϕ_i, and the influence of the scalar field is visible only through the pre factor in (5.3).

In the general model, with a massive scalar field, we have seen that in our range of interest, that is, large S, there is also a pair of real Lorentzian classical solutions, for each value of S (and ϕ_b). The semiclassical wavefunction associated with both solutions has an oscillating behaviour as required in order to predict classical spacetime for the late universe. In Figures 4,5, and 6 we show the numerically calculated semiclassical wavefunctions associated with simplicial geometries that are cones over triangulations of some of the most relevant spatial $3-D$ universes, namely simple triangulations of the 3−sphere S^3, of $S^2 \times S^1$, and T^3, in the presence of massive scalar fields. The results clearly indicate an oscillatory behaviour for large S, signalling classical spacetime, in all cases. In the case of T^3, $S_{crit} < 0$, which means that the semiclassical wavefunction is valid for all values of S, and not just large ones. Similar calculations for other triangulations of the spatial $3-D$ universe yield similar wavefunctions, confirming the generality of the result.

6 Steepest Descents Contours

We will now investigate under what conditions the semiclassical approximation is a good approximation of the full wavefunction. Mathematically this happens when the contour of integration C can be distorted such that it passes as a steepest descent contour C_{SD} through the classical solutions (on which we wish to base our semiclassical approximation) so that the integral is dominated by the contribution from the neighbourhoods of those solutions.

In order to guarantee that this is indeed the case, a detailed knowledge of the entire

contour of integration is not necessary. It is sufficient to have such a knowledge near the extrema that supposedly dominate the integral, and prove that the integrand is sharply peaked around the classical solutions and that there are no other "critical points" yielding significant contributions to the integral.

In our model there are two integration variables ξ and ϕ_i and the full wavefunction of the universe is given by (3.5). We work under the assumption that ϕ_i is to be integrated over real values, and ξ over the complex Riemann surface of the Euclidean action I. In order to justify the validity of the semiclassical approximation for such wavefunction we need to prove that the integral over ξ, can be calculated as a steepest descent (SD) integral for all the relevant values of ϕ_i.

Assuming that this is true, we can replace $\int_{C_{SD}} d\xi e^{-I}$ by its semiclassical approximation based on the relevant classical extrema. This will give rise to Laplace type integrals in ϕ_i, when the extrema have real Euclidean action, and to Fourier type integrals in ϕ_i, when the extrema have pure imaginary Euclidean action. These integrals can then be shown to be dominated by the stationary points of the integrand which coincide with the classical solutions $\overline{\phi}_i$, where

$$\frac{\partial I[\overline{\xi}, \phi_i]}{\partial \phi_i} \mid_{\phi_i = \overline{\phi}_i} = 0$$

This justifies the validity of the semiclassical approximation to the full wavefunction.

In general, a SD contour associated with an extremum ends up either at ∞ or at a singular point of the integrand, or at another extremum with the same value of $Im(I)$. We have seen that in all three models considered, i.e., pure gravity, massless scalar field, and massive scalar field, when S is big enough the only classical solutions are a pair or real Lorentzian solutions $(\overline{\xi}_I(S, \phi_b), \overline{\phi}_i(S, \phi_b))$ and $(\overline{\xi}_{II}(S, \phi_b), \overline{\phi}_i(S, \phi_b))$, where $\overline{\xi}_I = \overline{\xi}_{II} < 1/4$. They are located on the first and second sheets respectively, and so have pure imaginary actions of opposite sign. Given that their actions are different valued no single SD path can go directly from one to the other extremum. On the other hand given that

$$I[\overline{\xi}, \phi_b] = [I[\overline{\xi}^*, \phi_b]]^*$$

and

$$I[\overline{\xi}_I, \phi_b] = -I[\overline{\xi}_{II}, \phi_b]$$

where $*$ denotes complex conjugation, we see that the SD path that passes through $\overline{\xi}_{II}$

will be the complex conjugate of the SD path that passes through $\overline{\xi}_I$. So the total SD contour will always be composed of two complex conjugate sections, each passing through one extremum, and this together with the real analyticity of the action guarantees that the resulting wavefunction is real.

6.1 Pure Gravity Model

In the pure gravity model the only singularity is located at $\xi = 1/3$, where $Im(I)$ diverges and so no SD contour that passes through a classical solution can end up at such a singularity. So in this model the SD paths passing through both classical Lorentzian extrema are condemned to end up at infinity. So we only have to worry about convergence of the integral when $\xi \to \infty$.

The appropriate SD contour for $S > S_{crit}$

$$C_{SD}(S) = \left\{ \xi \in R : Im[I(S,\xi)] = \tilde{I}[\overline{\xi}(S)] \right\} \tag{6.1}$$

(where R is the Riemann sheet of the action), can be shown to be made up of two sections, one passing through the Lorentzian extremum in the first sheet and the other its complex conjugate, passing through the extremum located in the second sheet.

For the SD path associated with $\overline{\xi}_I$ starting off in the first sheet the SD contour on the upper half of this sheet is given asymptotically by

$$\frac{a_3}{H^2} S(S - S_{crit}) Im(\sqrt{\overline{\xi}}) = \tilde{I}[\overline{\xi}_I] \tag{6.2}$$

and we can guarantee the convergence of the integral along this part of the SD contour because the real part of the action is asymptotically

$$Re[I(\xi, S)] \sim \frac{a_3}{H^2} S(S - S_{crit}^{m=0}) \sqrt{\mid \xi \mid} \tag{6.3}$$

The SD contour then passes through $\overline{\xi}_I \in (-\infty, 1/4]$ crossing into the second sheet of the action. Proceeding along the SD contour we will then transverse the branch cut $(-\infty, 3/8]$, again. When S is sufficiently large, the crossing happens between $1/4$ and $1/3$, and we emerge in the third sheet. If S is smaller, the crossing happens between $1/3$ and $3/8$, and we emerge in a different sheet, but the asymptotic behaviour of the action is similar and so in terms of the convergence of the integral, the two situations are equivalent. In the third

sheet the SD contour then proceeds to infinity in the first quadrant along the curve that is asymptotically defined by

$$\frac{a_3}{H^2} S(S + S_{crit}^{IIIm=0}) Im(\sqrt{\xi}) = \tilde{I}[\overline{\xi}_I] \tag{6.4}$$

Once again the convergence is guaranteed by the asymptotic behaviour of the action

$$Re[I(\xi, S)] \sim \frac{a_3}{H^2} S(S + S_{crit}^{IIIm=0}) \sqrt{\mid \xi \mid} \tag{6.5}$$

Figure 7 shows a numerical computation of such an SD contour for the case of $\mathcal{M}^3 = T^3$.

The asymptotic behaviours of the two sections are such that they meet at infinity on the first and third sheets, thus obtaining a closed SD contour defining the wavefunction of the universe.

The SD integral over ξ is thus well approximated by the semiclassical approximation associated with these two Lorentzian extrema and so it yields a wavefunction that in the late universe (large S) predicts classical Lorentzian spacetime that is a solution of the Einstein GR equations, as desired.

6.2 Massless Scalar Field model

In the massless scalar field model, the situation is somewhat different. There is a second integration on the variable ϕ_i. So if in the previous case we had a family of SD contours labelled by the value of S we now have a family of SD contours labelled by two variables, namely S and $\phi_i - \phi_b$.

$$C_{SD}(S, \phi_i - \phi_b) = \left\{ \xi \in R : Im[I(S, \xi, \phi_i - \phi_b)] = \tilde{I}[\overline{\xi}(S, \phi_b), \overline{\phi}_i = \phi_b)] \right\} \tag{6.6}$$

where R is the Riemann sheet of the action.

We must be able to obtain the SD contour in ξ for each value of S and $\phi_i - \phi_b$, and prove that it verifies the conditions mentioned above for all relevant values of ϕ_i and S. The numerical computation of these steepest descent contours, for values $S > S_{crit}^{IIIm=0}$, yields two different kinds of contours. For large enough values of S, the SD contours for each value of $\phi_i - \phi_b$, are similar to the SD contours we have encountered in the pure gravity model. See Figure 8.

The fact that the asymptotic behaviour of the action is the same in both the pure gravity model and the massless scalar field model guarantees the convergence of the SD contour.

However, when the value of S is smaller the influence of the singularity at $\xi = 0$ dominates and we obtain a different kind of SD contour. In Figure 9 we show the SD contour for a cone over the 3−sphere triangulation α_4, passing through the classical Lorentzian solution located in the first sheet, $\overline{\xi}_I$, when $S = 50$ and $\phi_i - \phi_b = 5$

We see that instead of the SD contour going off to infinity in the first quadrant of the first sheet, like in the previous model, it is now shifted towards $\xi = 0$ by the singularity that exists there.

This is possible because as $\xi \to 0$ along the SD contour, the imaginary part of the action remains constant while the real part diverges to $+\infty$,

$$Re[I(\xi, S, \phi_i, \phi_b)] \to \frac{S}{H^2}\Big(\frac{N_3}{160\sqrt{3}}\Big)(\phi_i - \phi_b)^2 \mid \xi \mid^{-1} \tag{6.7}$$

Thus the contribution of the singularity to the SD integral is vanishing.

As we pass through the Lorentzian classical solution $\overline{\xi}_I \in (-\infty, 1/4]$ we emerge into the second sheet. From then on the behaviour of the SD contour is very similar to the one in the pure gravity model. There is a second branch cut crossing somewhere between 1/4 and 3/8, (according to the value of S), and the SD contour then proceeds to infinity along the third sheet. Again, since the asymptotic behaviour of the action in the massless field models and in the pure gravity models is the same, the localisation of the contours and the behaviour of the real part of the action will be common to both models, and that guarantees the convergence of the SD integral in the massless scalar field models.

Obviously as in the previous model, the total SD contour also includes a similar SD contour (complex conjugate) for the other classical Lorentzian solution, located on the second sheet, ensuring that the resulting wavefunction is real.

6.3 Massive Scalar Field Model

Although, as in the massless case, we now have a different SD contour for each value of S, ϕ_b and ϕ_i, an appropriate SD contour leading to a Lorentzian classical spacetime can always be found, for each value of ϕ_i. We are mainly interested in what happens for large values of S, for which there is a pair of Lorentzian classical solutions $\{\overline{\xi}_k(S, \phi_b), \overline{\phi}_i^k(S, \phi_b)\}, k = I, II$, for every value of S and ϕ_b. Figures 10, 11, and 12 show the results of our numerical computation of the SD contour passing through the classical Lorentzian solution on the first sheet, $\overline{\xi}_I$, in the case of a cone over α_4, $\mathcal{S}^2 \times \mathcal{S}^1$, and $\mathcal{T}^3$, for $S = 100$, $\phi_b = 1$ and $m = 1$.

They all have similar behaviours, and so we shall concentrate on the α_4 case, in figure 10. Proceeding upward from the extremum, $\overline{\xi}_I(S = 100, \phi_b = 1) = 0.2114$ the SD contour proceeds to infinity along the first quadrant of the plane, along the parabola

$$\frac{a_3 + A(\phi_i, \phi_b)}{H^2} S(S - S_{crit}) Im(\sqrt{\xi}) = \tilde{I}[\overline{\xi}_I, \overline{\phi_i}] \tag{6.8}$$

The convergence of the integral along this part of the contour is guaranteed by the asymptotic behaviour of the action along the SD contour on the first sheet

$$Re[I^I(\xi, S, \phi_i, \phi_b)] \sim \frac{a_3 + A(\phi_i, \phi_b)}{H^2} S(S - S_{crit}) \sqrt{\mid \xi \mid} \tag{6.9}$$

Moving downward from the extremum at $\overline{\xi}_I = 0.2114$, we immediately cross the branch cut and hence emerge onto the second sheet. Once again due to the alteration of the sign of the action one cannot proceed immediately to infinity. Instead the SD contour crosses the branch cut once more at $\xi = 0.2763$ between 1/4 and 1/3, emerging onto the third sheet, where it finally proceeds to infinity in the first quadrant of this third sheet along

$$\frac{a_3 + A(\phi_i, \phi_b)}{H^2} S(S + S^{III}_{crit}) Im(\sqrt{\xi}) = \tilde{I}[\overline{\xi}_I, \overline{\phi_i}] \tag{6.10}$$

Once more convergence is a consequence of the asymptotic behaviour

$$Re[I^{III}(\xi, S, \phi_i, \phi_b)] \sim \frac{a_3 + A(\phi_i, \phi_b)}{H^2} S(S + S^{III}_{crit}) \sqrt{\mid \xi \mid} \tag{6.11}$$

As before, the SD contour that passes through the other extremum located in the equivalent position, $\overline{\xi}_{II} = 0.2114$, but in the second sheet, is the complex conjugate of the previous contour, and the full SD contour is then taken to be the union of these two sections. Thus we see that the semiclassical approximation based on these two Lorentzian classical solutions can be justified in all three cases by the existence of these SD contours.

Note that although we only present the results for the most significant topologies the same computations can be performed for any other simplicial spacetime that is a cone over a closed, connected combinatorial 3−manifold. We only have to change the values of N_1 and N_3 accordingly.

7 Conclusions

Having emphasised the need to consider more general spacetimes, other than the ones that are classical solutions of Einsteins' equations, i.e., manifold-based spacetimes, we then proceeded to show that the contributions for the wavefunction of the universe coming from some of these non-manifold based spacetimes are still consistent with a wavefunction predicting classical spacetime for the late universe, in accordance with our everyday experience. In order to have a finite representation of these spacetimes we appealed to the simplicial representation of topological spaces and the Regge calculus formulation in order to specify the simplicial metric on those simplicial complexes.

By considering only complexes of cone-like type (combinatorial conifolds), a natural minisuperspace approximation arises, with only one internal metric degree of freedom. To make it somewhat more realistic we also considered the presence of a massive scalar field.

Proving the existence of convergent steepest descent contours of integration associated with Lorentzian classical solutions for each case, we justified the validity of the semiclassical approximation for the minisuperspace wavefunctions associated with our models. The resulting wavefunctions do indeed exhibit an oscillatory behaviour for the late universe, consistent with the prediction of Lorentzian classical spacetime as we know it.

These results add credibility to the generalization of the concept of history in the sum over histories formulation of quantum gravity to include more general, non-manifold based histories, in particular conifold based histories. Conifolds are particularly suitable for our objectives because although more general than manifolds they are still regular enough for all the usual basic concepts in GR to be easily extended to them. On the other hand their situation concerning algorithmic decidability is more favourable than that of manifolds because the set of closed connected $4-$conifolds is known to be algorithmically decidable, which is still an open problem for $4-$manifolds.

Finally, it should be noted that of the three conditions that any contour of integration should verify, the SD contours we have calculated only explicitly obey two of them, namely, convergence and leading to a wavefunction predicting classical space-time when the universe is large. We have not concerned ourselves with what regards the satisfaction of the constraints implementing diffeomorphism invariance, the status of which is still not fully understood in the simplicial framework [13]. However we expect the minisuperspace approximation to be a good testing ground for further study.

Acknowledgements

The authors thank Kristin Schleich for helpful discussions and advice. The work of C. Correia da Silva was supported by the Portuguese Ministry of Science and Technology under grant PRAXIS XXI BD-5905/95. Other support has come from the UK Particle Physics and Astronomy Research Council.

References

[1] J.B.Hartle, Class.Quantum Grav.**2** (1985) 707.

[2] K. Schleich and D.M. Witt, Nucl. Phys. B**402** (1993) 411 and 469.

[3] J.B.Hartle, J.Math.Phys **26** (1985) 804.

[4] J.B.Hartle, J.Math.Phys **30** (1989) 452.

[5] D.Birmingham, Phys.Rev.D**52** (1995) 5760.

[6] J.Louko and P.A.Tuckey, Class.Quantum Grav.**9** (1992) 41.

[7] R.M. Williams and P.A.Tuckey, Class.Quantum Grav.**9** (1992) 1409.

[8] Y.Furihata, Phys.Rev.D**53** (1996) 6875.

[9] H.W.Hamber and R.M.Williams, Nucl.Phys.B**415** (1994) 463.

[10] J.B.Hartle and S.W.Hawking, Phys.Rev.D**28** (1983) 2960.

[11] W.Kuhnel, *Triangulations of Manifolds with Few Vertices*, in *Differential Geometry and Topology*, ed. F. Tricerri, World Scientific, Singapore, 1990.

[12] J.J. Halliwell and J.B. Hartle, Phys.Rev.D**41** (1991) 1815.

[13] R.M. Williams, Nucl.Phys.Proc.Suppl.**57** (1997) 73.

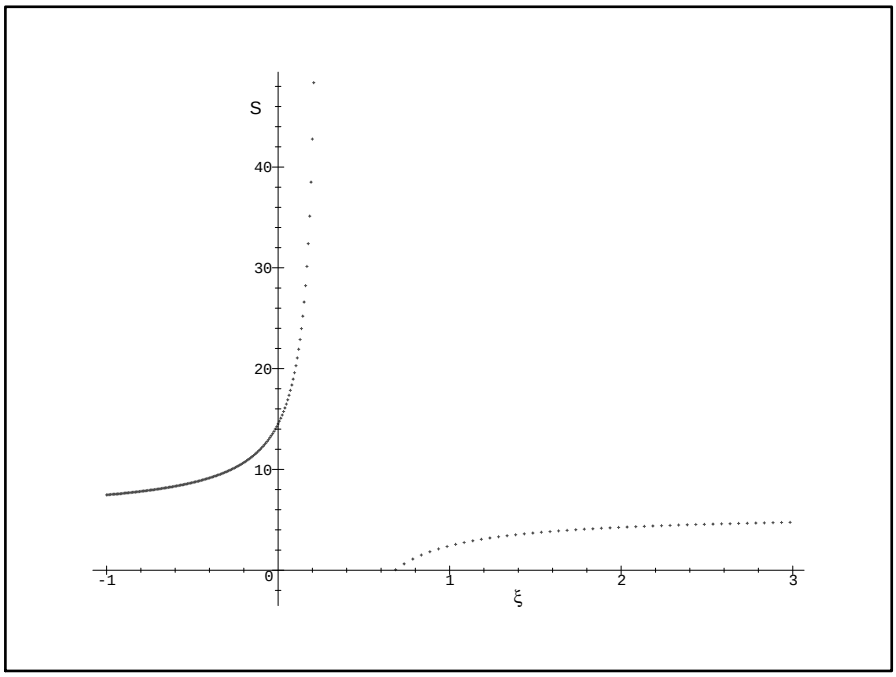

Figure 1: Classical solution for the cone over the triangulation $\mathcal{S}^2 \times \mathcal{S}^1$

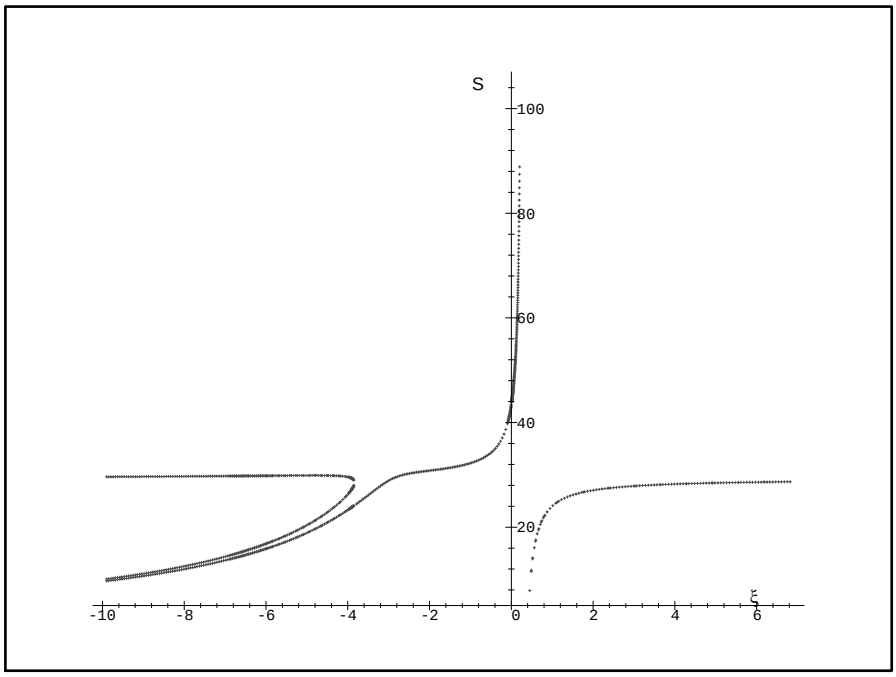

Figure 2: Classical solution for the cone over the triangulation α_4 with a scalar field of mass $m = 1$ and $\phi_b = 1$

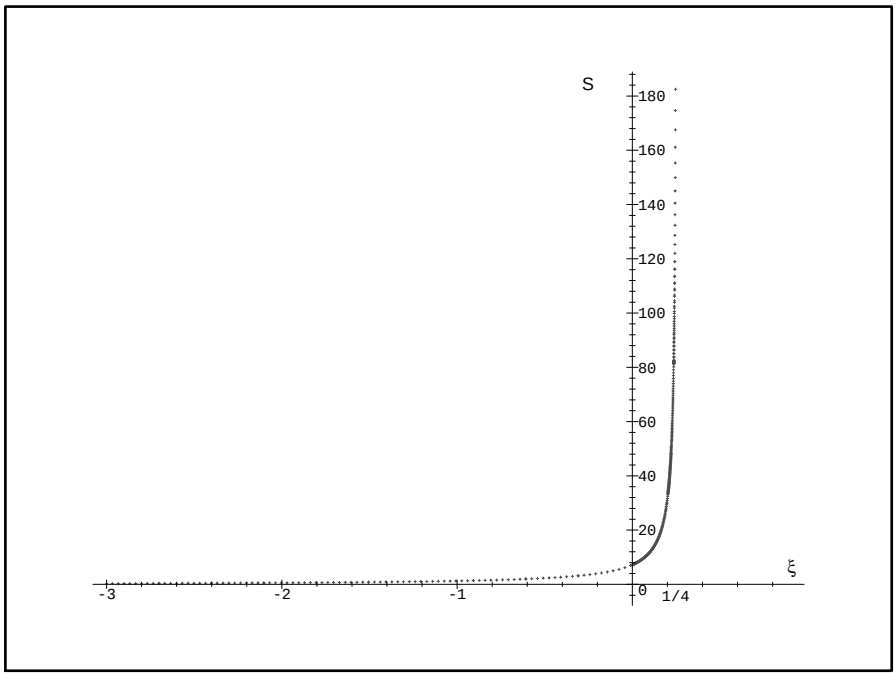

Figure 3: Classical solution for the cone over the triangulation $\mathcal{T}^3$ with a scalar field of mass $m = 1$ and $\phi_b = 1$

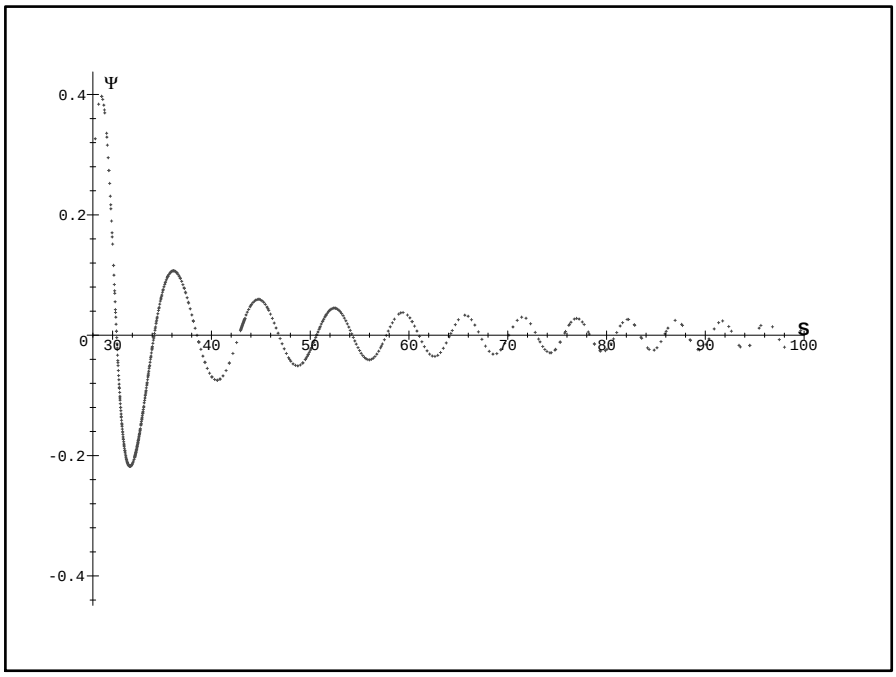

Figure 4: Semiclassical wavefunction for a cone over α_4 with scalar field of mass $m = 1$ and $\phi_b = 1$, for $H = 7$.

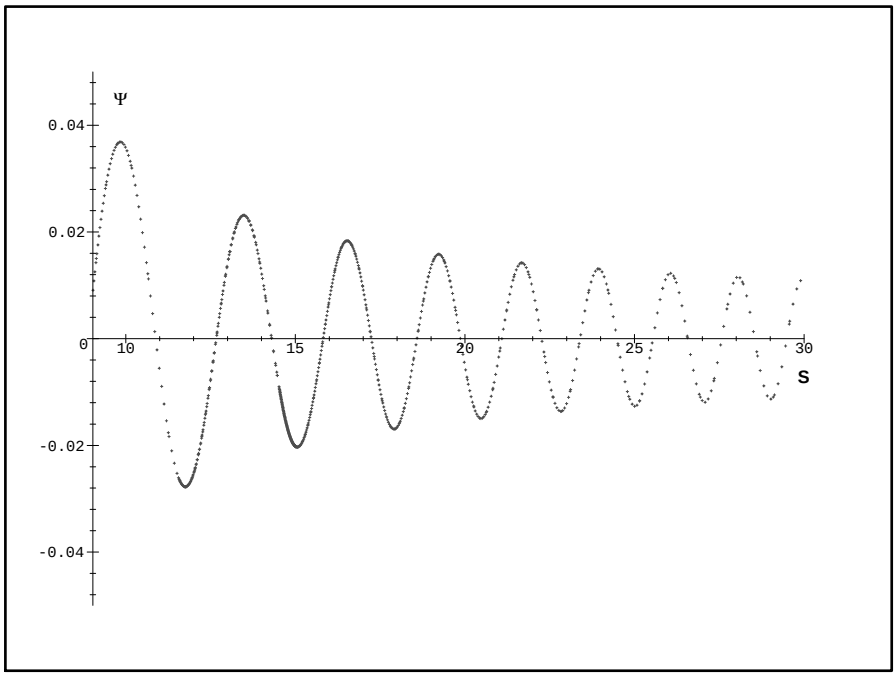

Figure 5: Semiclassical wavefunction for a cone over $\mathcal{S}^2 \times \mathcal{S}^1$ with scalar field of mass $m = 1$ and $\phi_b = 1$, for $H = 7$.

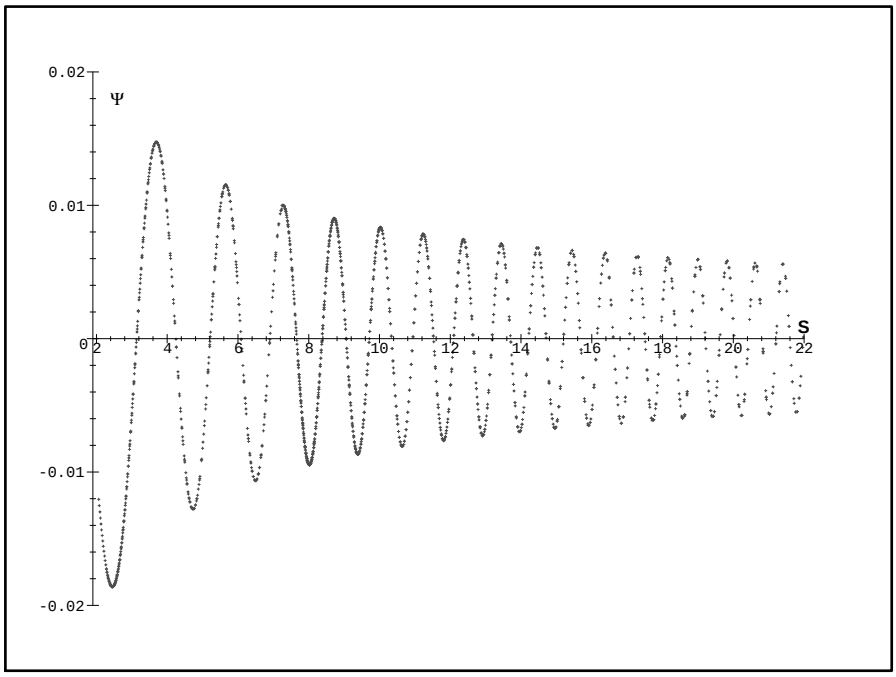

Figure 6: Semiclassical wavefunction for a cone over $\mathcal{T}^3$ with scalar field of mass $m = 1$ and $\phi_b = 1$, for $H = 7$.

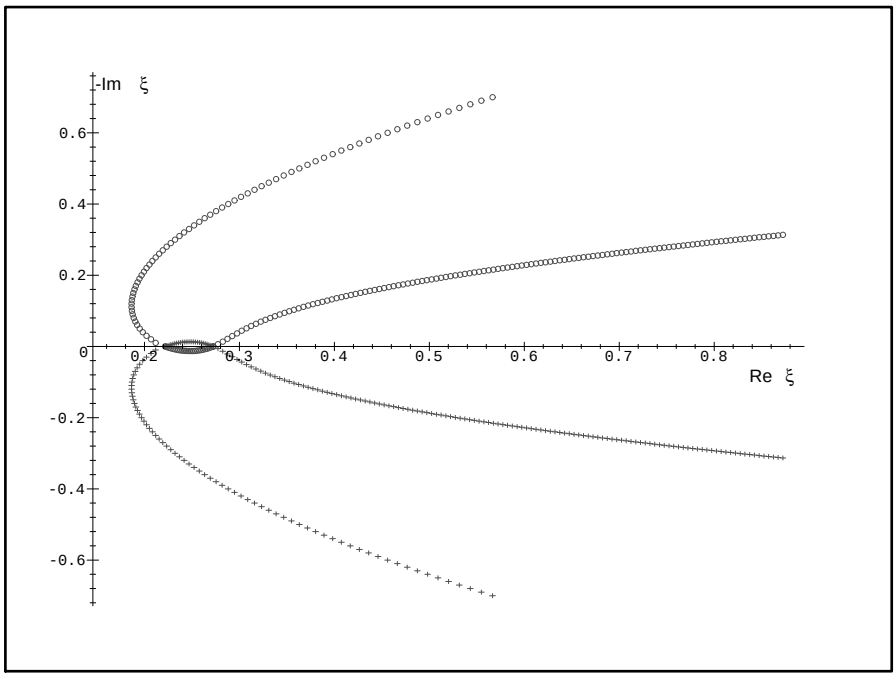

Figure 7: Steepest descents contour for a cone over $\mathcal{T}^3$ with $S = 50$. Note that unlike the next figures we present both sections of the SD contour. The section associated with the extremum in the first sheet (at $\xi = 0.2218$), is represented by the circle-like points, and the other section passing through the second extremum located in the same position but in the second sheet is represented by the cross-like points. In both cases the contours cross the branch cut again at $\xi = 0.2724$, between the branch points $1/4$ and $1/3$ before proceeding to infinity.

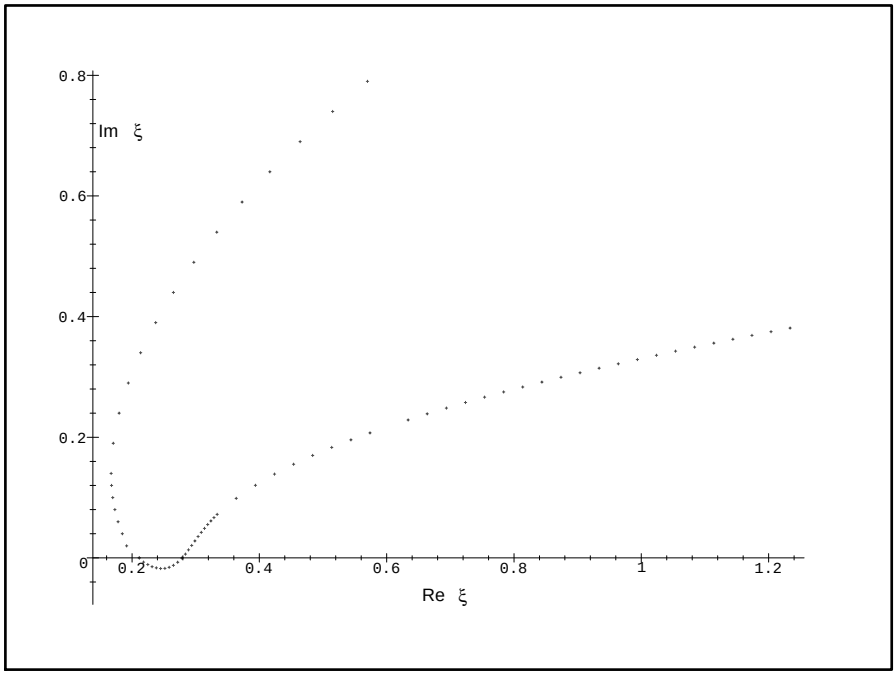

Figure 8: Steepest descents contour for a cone over α_4 with a massless scalar field taking value $\phi_i - \phi_b = 0.1$ and $S = 100$. Starting at infinity in the first sheet it passes through the real extremum at $\xi = 0.2114$, goes into the second sheet and crosses again the branch cut at $\xi = 0.2788$, between $1/4$ and $1/3$ thus emerging onto the third sheet where it proceeds to infinity. Note that this behaviour is maintained for any larger value of S.

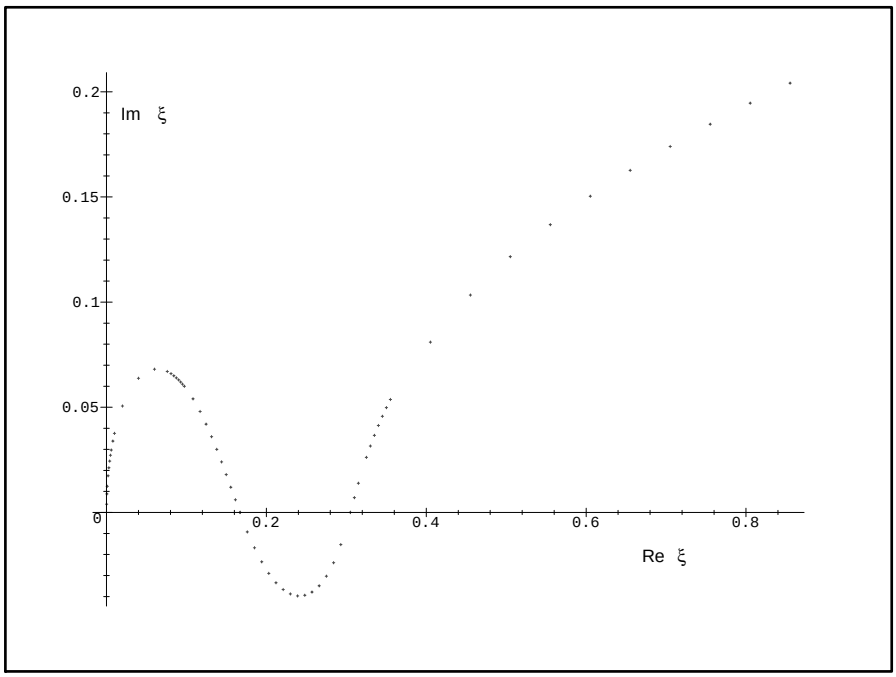

Figure 9: Steepest descents contour for a cone over α_4 with a massless scalar field taking value $\phi_i - \phi_b = 5$ and $S = 50$. Moving upward from the real extremum in the first sheet located at $\xi = 0.1671$, instead of going to infinity it is attracted into the singularity at $\xi = 0$. Moving downward it goes into the second sheet later emerging onto the third sheet crossing the branch cut at $\xi = 0.3052$, between the branch points at $1/4$ and $1/3$, and proceeding to infinity

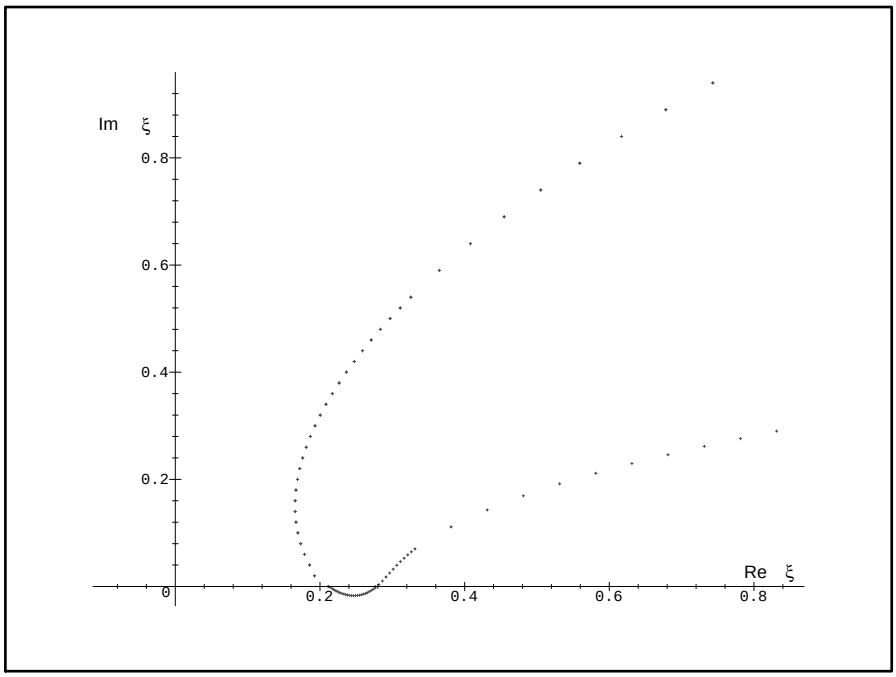

Figure 10: Steepest descents contour for a cone over α_4 with scalar field of mass $m = 1$ with $\phi_b = 1$ and $S = 100$, when $\phi_i - \phi_b = 2$. Starting at infinity in the first sheet it passes through the real extremum at $\xi = 0.2114$, goes into the second sheet and crosses again the branch cut at $\xi = 0.2763$, between 1/4 and 1/3 thus emerging onto the third sheet where it proceeds to infinity.

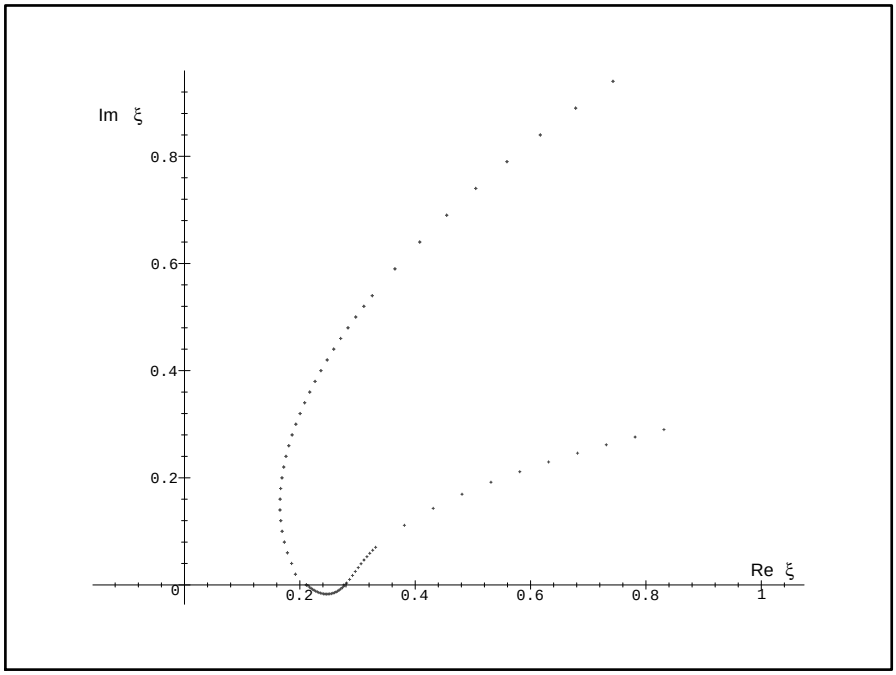

Figure 11: Steepest descents contour for a cone over $\mathcal{S}^2 \times \mathcal{S}^1$ with scalar field of mass $m = 1$ with $\phi_b = 1$ and $S = 100$, when $\phi_i - \phi_b = 0.1$. Starting at infinity in the first sheet it passes through the real extremum at $\xi = 0.2356$, goes into the second sheet and crosses again the branch cut at $\xi = 0.2628$, between 1/4 and 1/3 thus emerging onto the third sheet where it proceeds to infinity.

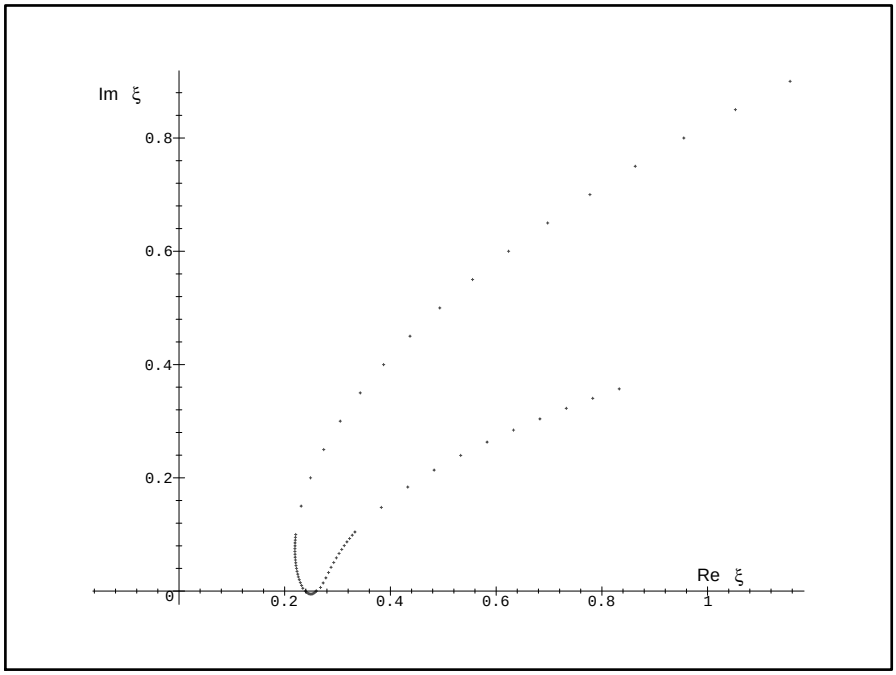

Figure 12: Steepest descents contour for a cone over $\mathcal{T}^3$ with scalar field of mass $m = 1$ with $\phi_b = 1$ and $S = 100$, when $\phi_i - \phi_b = 0.1$. Starting at infinity in the first sheet it passes through the real extremum at $\xi = 0.2393$, goes into the second sheet and crosses again the branch cut at $\xi = 0.2598$, between 1/4 and 1/3 thus emerging onto the third sheet where it proceeds to infinity.